Madelung−Buckingham Model as Applied to the Prediction of Voltage, Crystal Volume Changes, and Ordering Phenomena in Spinel-Type Cathodes for Lithium Batteries

Daniel Sherwood, K. Ragavendran, and Bosco Emmanuel*

Modeling and Simulation Group, Central Electrochemical Research Institute, Karaikudi 630006, India

Received: February 18, 2005; In Final Form: May 4, 2005

Using a Madelung−Buckingham model, we study $Li_xMn_2O_4$ and its fluorine-substituted analogue to compute their voltages, lattice volume changes, and ordering phenomena during charge/discharge. The interactions included are the long-range Coulombic, short-range electron−electron repulsion, and the van der Waals. The voltage of the fluorine-substituted spinel is found to be slightly less than that of the unsubstituted. However, the former undergoes a greater crystal volume change than the latter during intercalation and de-intercalation. Investigations of lithium sublattice ordering in this system indicates that during intercalation lithium starts filling exclusively into one sublattice until $x = 0.5$, and only from $x = 0.5$ the other sublattice is filled up to $x = 1$. The models are compared with quantum ab initio and experimental results.

1. Introduction

Computer-aided simulations for the prediction of voltages and lattice volume changes of cathode materials during charge/discharge are being carried out by several researchers across the globe. Gao, Reimers, and Dahn[1] have used mean-field approximation and Newman et al.[2] use Monte Carlo simulation to predict the voltages of spinel-type cathode materials using a lattice gas model that is well-known in statistical mechanics. This model uses two parameters, nearest neighbor and next-nearest neighbor interactions. These interaction parameters are obtained a posteriori by fitting with experiment, thereby making them lose their quantitative predictive power, though they give some useful insights. On the other hand, the state-of-the-art quantum ab initio methods demand huge computational resources. Ceder et al.[3,4] employing these methods in particular to layered systems such as Li_xCoO_2 have used a Cray C90 supercomputer. Even such huge computational resources are inadequate to study the cathodes at intermediate charge states and with substituents. Hence, we embark upon a program based on classical physics and develop models that provide a PC-based solution for computing material properties in lithium batteries. We earlier used a Madelung model to compute the voltage of lithium manganate,[5] which is summarized in section 2. In this paper, we extend our theory using a Madelung−Buckingham model to study the voltage and lattice volume changes in $Li_xMn_2O_4$ (section 3) and $Li_xMn_2O_{4-z}F_z$ (section 4). Ordering phenomena in $Li_xMn_2O_4$ are dealt with in section 5.

2. Madelung Model and Battery Voltages

The cohesive energy of an ionic solid consists mainly of the long-range Coulomb interactions among its constituent ions, with short-range electron−electron repulsion (Born interaction) and van der Waals-type multipolar interactions contributing 10−12%. It may be pointed out here that all of these interactions share the same electrostatic origin and we have separated the various interactions only for the convenience of representing them.

$$\text{cohesive energy of an ionic solid} = (90\%)E_M + (\sim 10\%)E_S + (1\%)E_{MP} \quad (1)$$

where E_M, E_S, and E_{MP}, respectively, denote the long-range ion−ion interaction or the Madelung energy, the short-range electron−electron repulsion, and the multipolar contributions.

The Madelung energy E_M for nonstoichiometric and variable-valent compounds can be given by the formula

$$E_M = {}^1/_2[\sum_{g\neq 0}(S\cdot S^*)f(g) + \{\sum_{i=1}^{N}\lambda^2(i)\}.F(G) + \sum_{j=1}^{N}\lambda(j)\sum_{i\neq j}^{N}\lambda(i)\bar{F}(G,\mathbf{r}_i^j)] \quad (2)$$

Reference 5 may be consulted for the notations in eq 2.

Execution of eq 2 required the following inputs to our program: the space group of the material, the lattice constants, and the atomic positions of ions in the primitive cell. The convergence factor G is normally set as 1 with a grid size of $10 \times 10 \times 10$ for both direct and reciprocal lattices.

2.1. Calculation of Battery Voltage. The net energy $\Delta E(x)$ for the discharge reaction $x\text{Li(s)} + Mn_2O_4 \rightarrow Li_xMn_2O_4$ can be obtained[5] by breaking the reaction into elementary Born steps.

$$\Delta E(x) = {}^1/_8[x(1.65 + 5.34) - x(52) - E_M(Mn_2O_4) + E_M(Li_xMn_2O_4)] \quad (3)$$

$$\Delta E(x) = {}^1/_8[x(1.65 + 5.34) - x(52) - E_M(Mn_2O_{3.8}F_{0.2}) + E_M(Li_xMn_2O_{3.8}F_{0.2})] \quad (4)$$

The Battery voltage can be given in terms of $\Delta E(x)$ by the formula

$$V = -(1/F)\, d[\Delta E(x)]/dx \quad (5)$$

* Author to whom correspondence should be addressed. E-mail: boscok@rediffmail.com.

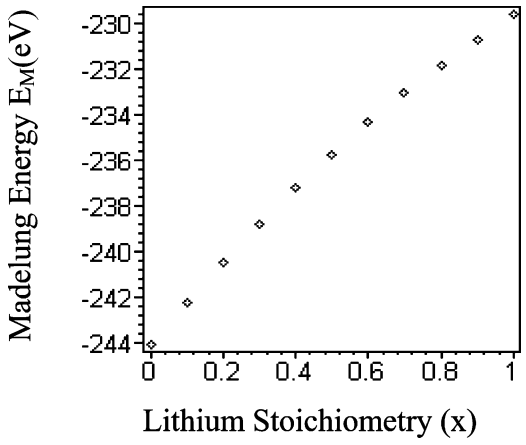

Figure 1. Madelung energy E_M (in eV/formula unit) versus the stoichiometry x (from ref 5).

TABLE 1: Results of Voltage Prediction for Pristine and Fluorine-Substituted Lithium Manganate

cathode system	method of voltage estimation	voltage
$Li_xMn_2O_4$	experiment[6]	4.1
$Li_xMn_2O_4$	Madelung model	4.042
$Li_xMn_2O_4$	Madelung−Buckingham model	3.9
$Li_xMn_2O_4$	Madelung−Buckingham model + lattice distortion	3.88
$Li_xMn_2O_4$	quantum ab initio[3]	3.9
$Li_xMn_2O_{3.8}F_{0.2}$	experiment	*a*
$Li_xMn_2O_{3.8}F_{0.2}$	Madelung−Buckingham model + lattice distortion	3.876

[a] Not available.

A typical plot of the Madelung energy E_M versus the Li stoichiometry x is given in Figure 1.

Through the use of eq 5, the battery voltage turns out to be 4.042 V for $Li_xMn_2O_4$. The effect of other interactions such as short-range electron−electron repulsion and lattice distortions on the battery voltage is low. Table 1 summarizes the results of the voltage prediction of lithium manganate through various models and compares them with the experimental results.[6] We note from Table 1 that the Madelung model prediction of battery voltage is closer to the experimental value than the prediction of its extension. Presently, we do not understand the reason for this. (It is interesting to note here that the ab initio quantum computation[3] for $Li_xMn_2O_4$ predicts the same voltage as the Madelung−Buckingham model.) However, the primary goal for the model extension is to incorporate the crystal volume changes to which we turn in the next section.

3. Madelung−Buckingham Model and Crystal Volume Changes

Lithium manganate is an important cathode material in lithium battery applications. Though it is less expensive and more eco-friendly in comparison to other cathode materials such as lithium cobaltate (Li_xCoO_2), $Li_xMn_2O_4$ suffers from capacity losses[7] that are of two kinds: reversible capacity loss and irreversible capacity loss. The reversible capacity loss arises from the low mobility and hence long diffusion path lengths for Li-ion transport in the lithium manganate crystallites. Reversible capacity loss can, in principle, be minimized at smaller currents and over a larger discharge time. Irreversible capacity loss is related to (i) manganese dissolution from the $Li_xMn_2O_4$ cathode in the battery electrolyte[8] and (ii) volume changes in the host lattice upon charge/discharge. It is the capacity loss under category (ii) that the present paper is concerned with**.** This irreversible capacity loss arises as follows: the lithium battery cathode of our interest here is a composite film consisting of $Li_xMn_2O_4$ particles interspersed with particles of carbon powder. $Li_xMn_2O_4$ is a poor electrical conductor, and the carbon particles that sit between the $Li_xMn_2O_4$ crystallites help to improve the electrical conductivity of the composite film.[9] However, upon being charged, lithium is de-intercalated from the $Li_xMn_2O_4$ particles, leading to a decrease in their crystal volume, and on being discharged, lithium is re-intercalated, and the crystal volume increases. Hence, when the battery is repeatedly charged and discharged, the lithium manganate particles expand and contract, which results in an irreversible loss of interparticle contacts and hence the increased capacity loss of the composite cathode film.

Cyclability of $Li_xMn_2O_4$ is determined by the structural integrity of the host lattice.[10] Minimizing the crystal volume change on charge/discharge will, therefore, greatly enhance the performance of the cathode. In this section, we use a Madelung−Buckingham model to theoretically simulate the variation of the cubic lattice constant of $Li_xMn_2O_4$ during charge/discharge. Although we have applied the model to $Li_xMn_2O_4$ and $Li_xMn_2O_{3.8}F_{0.2}$ in this paper, it can be applied to any ionic crystal amenable to a Madelung−Buckingham-type description. We propose that the model will be useful in screening them for their susceptibility to irreversible capacity loss due to crystal volume changes on charge/discharge.

Several recent references can be cited that make use of Buckingham-type multipolar interactions.[11−14] For evaluation of intermolecular interaction energies with pseudo-atom representations of molecular electron densities, the Buckingham-type model has been employed.[12] An atomistic simulation of the surface structure of wollastonite is also successfully implemented within the Buckingham-type approximation.[13] Oxygen ion mobility in yttria-stabilized zirconia has also been simulated using this model.[11]

3.1. Computational Details. The lattice constant a of the cubic crystal $Li_xMn_2O_4$ is that value of a that minimizes the crystal energy. The contribution to the total energy of a nonstoichiometric and variable-valent ionic crystal due to long-range interactions can be evaluated using the Ewald method.[5] Contributions from the short-range electron−electron repulsion and the van der Waals forces can be modeled using the Buckingham potential

$$A_{ij}\exp(-r_{ij}/\rho_{ij}) - C_{ij}/r_{ij}^{6} \tag{6}$$

and can be written as

$$E_B(x) = \sum_{(i,j)} N_{ij} f_i f_j \{A_{ij}\exp(-r_{ij}/\rho_{ij}) - C_{ij}/r_{ij}^{6}\} \tag{7}$$

where A_{ij}, ρ_{ij}, and C_{ij} are the relevant Buckingham parameters for the ion pair (i,j) and r_{ij} is the distance of separation. The ion pair (i,j) runs over the nearest neighbor and the next-nearest neighbor ion pairs, and f_i and f_j are the x-dependent occupancies at sites i and j, respectively. N_{ij} is the number of pairs of the type (i,j) per formula unit. Ammundsen and co-workers[15] have computed the Buckingham parameters A_{ij}, ρ_{ij}, and C_{ij} appearing in eq 6 from the vibrational spectra of $Li_xMn_2O_4$. Self-consistent interionic potentials have also been reported for a host of binary and ternary oxides by Bush et al.[16] These and other parameters used in the computation of eq 6 are listed in Table 2. Note also that the interionic distances r_{ij} can also be scaled by the lattice constant a and written as $r_{ij} = (r_{ij}/a)a$, where (r_{ij}/a) is a nondimensional constant, denoted $\bar{r}_{ij}$ in Table 2.

TABLE 2: Parameters Used for the Madelung−Buckingham Computation

ion pair (i,j)	N_{ij}	f_i	f_j	A_{ij} (eV)	ρ_{ij} (Å)	C_{ij} (eV Å^6)	$\bar{r}_{ij}$
$O^{2-}\cdots O^{2-}$	24	1	1	22764.3	0.149	43	0.3361
$Li^{+}\cdots O^{2-}$	4	x	1	426.48	0.300	0.0	0.2376
$Mn^{3+}\cdots O^{2-}$	12	$x/2$	1	1267.5	0.324	0.0	0.2381
$Mn^{4+}\cdots O^{2-}$	12	$(1 - x/2)$	1	1345.15	0.324	0.0	0.2381

The ion pairs in Table 2 are the nearest neighbor pairs. The next-nearest neighbor interaction was found to be significant, in addition to the first, for the $O^{2-}\cdots O^{2-}$ pair and was included in the computation, while for the other ion pairs the nearest neighbor interactions were adequate.

It may further be noted that for the cubic system $Li_xMn_2O_4$ the unit-cell constant a can be chosen as a convenient length scale, and hence, the Madelung energy can be expressed as

$$E_M(x) = -\frac{f(x)}{a} \tag{8}$$

where the function $f(x)$ depends only on the stoichiometry x and is independent of a.

Combining eqs 1, 7, and 8, we get

$$E(x,a) = E_M(x,a) + E_B(x,a) = -\frac{f(x)}{a} + \sum_{(i,j)} N_{ij} f_i(x) f_j(x) \{A_{ij} \exp(-\bar{r}_{ij} a/\rho_{ij}) - (C_{ij}/\bar{r}_{ij}^{\,6}) a^{-6}\} \tag{9}$$

It is to be noted that the total energy E depends on the lattice constant a in addition to the stoichiometry index x. For each value of x (in the range between 0 and 1), the value of a can be obtained by minimizing $E(x,a)$ with respect to a, i.e., $(\partial E(x,a)/\partial a) = 0$. Results of this minimization for several values of x are shown in Figures 2 and 3. The predicted variation of the lattice constant a with x is in excellent agreement with experimental data reported in the literature for $Li_xMn_2O_4$.[17] Moreover, it is interesting to note that the variation of a is linear in x, despite the nonlinearities manifest in eq 9.

Before we close this section, we wish to note that we have not included any size effects in our Madelung−Buckingham model based computations discussed above. We argue below that the size effect will not be important for particles of micron size. If we take a particle of micron size and the unit-cell dimension of the crystal as nearly 8 Å (as in the case of $Li_xMn_2O_4$), then we find that each micron-sized particle will have $\sim 10^9$ unit cells in it, and hence we are practically at the infinite limit. We do not even need as large a number as 10^9 to make our point. In a classic paper, Benson et al.[18] showed that for a droplet consisting of a close-packed cluster of only 13 atoms interacting via Lennard-Jones forces the surface tension is only 15% less than that of the infinite cluster. Another recent work is also worthy of mention here, where the authors[19] compute the Madelung energy and the lattice parameter of the nanocrystals of the fixed stoichiometry oxides CeO_2 and $BaTiO_3$ and find significant size effects only in the nanometer range. However, we do not consider nanoparticles in the present work. In contrast, what is of interest in our work is the effect of variable stoichiometry (i.e., state of charge of the battery) on the lattice parameter of micron-sized particles of the spinel $Li_xMn_2O_4$. The good agreement between our theoretical prediction and experimental data further proves that there is no size effect to worry about in our present work.

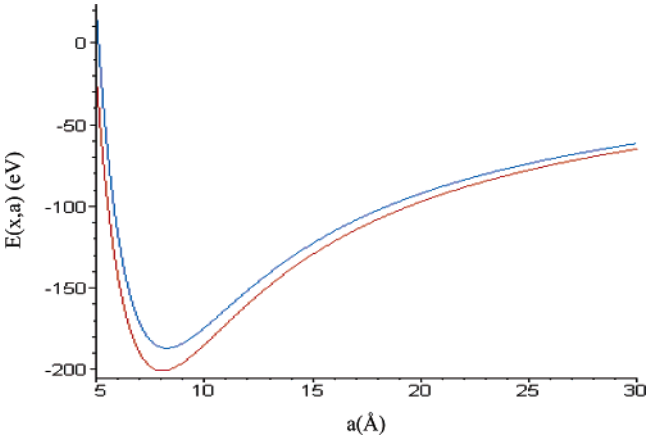

Figure 2. Energy $E(x,a)$ plotted versus a (red line for $x = 0$ and blue line for $x = 1$) for $Li_xMn_2O_4$.

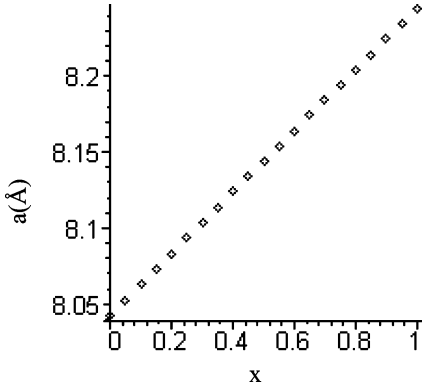

Figure 3. Equilibrium lattice constant a in angstroms versus the stoichiometry x for $Li_xMn_2O_4$.

4. Computation of Voltage and Crystal Volume Changes in $Li_xMn_2O_{3.8}F_{0.2}$ Using the Madelung−Buckingham Model

In this section, we use eq 9 to compute the voltage of $Li_xMn_2O_{4-z}F_z$. This fluorine-substituted lithium manganate is not yet reported in the literature. We were motivated to study the behavior of this hypothetical compound because O^{2-} and F^- are isoelectronic. Hence, fluorine substitution is expected to modify only the Madelung energy, and the short-range electron−electron repulsion and the van der Waals terms will remain essentially the same as that of O^{2-}. Hence, in Table 2, we have not separately included the interaction parameters for fluoride ion. The computational procedures and the parameters used in the calculation are similar to those adopted in section 3 except that $\lambda(i)$ is modified as follows

$$\lambda_1 = \lambda_2 = x$$

$$\lambda_3 = \lambda_4 = \lambda_5 = \lambda_6 = 4 - (x/2) - (z/2)$$

$$\lambda_7 = \lambda_8 \ldots = \lambda_{14} = -2 + (z/4)$$

where z is the atom fraction of fluorine.

The voltage of $Li_xMn_2O_{4-z}F_z$ turns out to be 3.876 V for $z = 0.2$. Table 1 compares the voltages of unsubstituted and fluorine-substituted spinels. The voltages are very similar, which is due to the fact that O^{2-} and F^- are isoelectronic. Minimization of $E(x,a)$ with respect to a was done for each value of x to obtain the equilibrium value of a. Figure 2 shows $E(x,a)$ versus a for $x = 0$ and $x = 1$ for $Li_xMn_2O_4$. Figure 3 shows the equilibrium lattice parameter a versus x for the same system.

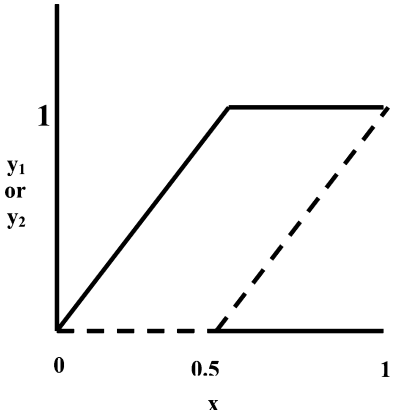

Figure 4. Sublattice occupancies (y_1,y_2) versus the state of charge x. Solid lines (—) represent filling of sublattice 1 and broken lines (- - -) represent filling of sublattice 2.

TABLE 3: Crystal Volume Changes for $Li_xMn_2O_{3.8}F_{0.2}$ and $Li_xMn_2O_4$

cathode system	a_0 (Å)	a_1 (Å)	Δa (Å)
$Li_xMn_2O_4$	8.045	8.2476	0.202
$Li_xMn_2O_{3.8}F_{0.2}$	8.148	8.3648	0.214

Our lattice volume computations on $Li_xMn_2O_{4-z}F_z$ signify that the crystal volume change (Δa) is greater in $Li_xMn_2O_{3.8}F_{0.2}$ than that in $Li_xMn_2O_4$ (Table 3), facilitating easier diffusion of lithium ions through the former.

5. Ordering Phenomena in Lithium Sublattices

The lithium manganate spinel consists of two interpenetrating face-centered cubic lithium sublattices. An atom in one sublattice will constitute the nearest neighbor to an atom in the other sublattice. In our earlier work,[5] to predict the voltage of Li_x-Mn_2O_4, we have assumed sublattice disorder, i.e., both the lithium sublattices can fill simultaneously so that we had assigned $\lambda_1 = \lambda_2 = x$ where x denotes the lithium stoichiometry. To make a study on sublattice ordering, we computed an energy matrix as a function of the lithium sublattice occupancies y_1 and y_2. From this matrix, we obtained by inspection the minimum energy state corresponding to each value of x and the corresponding sublattice occupancies. When we vary x from 0 to 1, it is found that up to $x = 0.5$ only one sublattice is taking up the lithium ions and that the other sublattice remains empty. In this range $y_1 = 2x$ and $y_2 = 0$. Only after crossing $x = 0.5$, the other sublattice (the sublattice with occupancy y_2) starts filling so that $y_1 = 1$ and $y_2 = 2x - 1$. Figure 4 gives a graphical description of this behavior. The occupancies y_1 and y_2 are related to x through the equation $(y_1 + y_2)/2 = x$. In previous studies,[1] similar ordering of the lithium sublattice has been found from lattice gas models. How the voltage is influenced by order−disorder transition is under investigation.

6. Conclusions

We have shown the applicability of our theory based on the Madelung−Buckingham model to predict the voltages, lattice constants, and ordering phenomena in $Li_xMn_2O_4$ and $Li_xMn_2O_{4-z}F_z$. The voltage of the fluorine-substituted analogue is very close to the pristine spinel, which is due to the fact that O^{2-} and F^- are isoelectronic. The fluorine-substituted spinel has a larger Δa, signifying easier diffusion of lithium through the spinel lattice. The results are in good agreement with experimental and quantum ab initio values for $Li_xMn_2O_4$. In comparison with quantum simulations, our classical simulations are not computationally very demanding. We were also able to compute voltages and lattice parameters for the cathode at the intermediate values of x using a 1.13 GHz Pentium III processor. Though the superiority of the ab initio methods must be admitted, currently available computational resources will not permit the quantum calculation of crystal volume changes for $Li_xMn_2O_4$. Hence, the classical method described in this paper is particularly attractive. The Madelung−Buckingham-type description and the Ewald method are well-known and widely employed. However, the present application to batteries is both new and interesting. Though we have illustrated this with the specific case of $Li_xMn_2O_4$, the proposed method applies equally well to a host of battery materials that are being actively studied. Studies on spinels of the type $Li_xMn_{2-y}M_yO_4$ (y = atom fraction of a metal substituent) are in progress in our lab. Our investigation showed the existence of sublattice order in the spinel system. The second sublattice of the spinel starts filling only after the first sublattice is completely filled. We also noticed that entropy has very little influence and it is only the energy part that plays a significant role in sublattice ordering.

Acknowledgment. We thank two anonymous referees for their useful comments on the manuscript.

References and Notes

(1) Gao, Y.; Reimers, J. N.; Dahn, J. R. *Phys. Rev. B* **1996**, *54*, 3878.
(2) Wong, W.; Newman, J. *J. Electrochem. Soc.* **2002**, *149*, 493.
(3) Van der Ven, A.; Marianetti, C.; Morgan, D.; Ceder, G. *Solid State Ionics* **2000**, *135*, 21.
(4) Ceder, G.; Chiang, Y. M.; Sadoway, D. R.; Aydinol, K. K.; Jang, Y. I.; Huang, B. *Nature* **1998**, *392*, 694.
(5) Ragavendran, K.; Vasudevan, D.; Veluchamy, A.; Emmanuel, B. *J. Phys. Chem. B.* **2004**, *108*, 16899.
(6) Amatucci, G.; Tarascon, J. M. *J. Electrochem. Soc.* **2002**, *149*, K31.
(7) Wang, E.; Ofer, D.; Bowden, W.; Iltchev, N.; Moses, R..; Brandt, K. *J. Electrochem. Soc.* **2000**, *147*, 4023.
(8) Lee, J. H.; Hong, J. K.; Jang, D. H.; Sun, Y. K.; Oh, S. M. *J. Power Sources* **2000**, *89*, 7.
(9) Dominko, R.; Gaberscek, M.; Drofenik, J.; Bele, M.; Pejornik, S.; Jamnik, J. *J. Power Sources* **2003**, *119*, 770.
(10) Thackeray, M. M. *J. Electrochem. Soc.* **1995**, *142*, 2558.
(11) Tang, Y. W.; Zhang, Q.; Chan, K. *Chem. Phys. Lett.* **2004**, *385*, 202.
(12) Volkov, A.; Koritsanszky, T.; Coppens, P. *Chem. Phys. Lett.* **2004**, *391*, 170.
(13) Kundu, T. K.; Rao, K. H.; Parker, S. C. *Chem. Phys. Lett.* **2003**, *377*, 81.
(14) Li, S.; Thompson, W. H. *Chem. Phys. Lett.* **2004**, *383*, 326.
(15) Ammundsen, B.; Burns, G. R.; Islam, M. S.; Kanah, H.; Roziere, J. *J. Phys. Chem. B* **1999**, *103*, 5175.
(16) Bush, T. S.; Gale, J. D.; Catlow, C. R. A.; Battle, P. D. *J. Mater. Chem.* **1994**, *4*, 831.
(17) *Lithium Ion Batteries: Fundamentals and Performance*; Wakihara, M., Yamamoto, O., Eds.; Wiley-VCH: Singapore, 1998; p 37.
(18) Benson, G. C.; Shuttleworth, R. *J. Chem. Phys.* **1951**, *19*, 130.
(19) Perebeinos, V.; Chan, S. W.; Zhang, F. *Solid State Commun.* **2002**, *123*, 295.